Second-harmonic generation sensitivity to transmembrane potential in normal and tumor cells

L. Sacconi
University of Trento
Department of Physics
via Sommarive 14
I-38050 Povo, Trento, Italy
and
European Laboratory for Non-linear Spectroscopy
via Nello Carrara 1
I-50019 Sesto Fiorentino, Florence, Italy

M. D'Amico
University of Florence
Department of Experimental Pathology and Oncology
viale Morgagni 50
I-50134 Florence, Italy

F. Vanzi
European Laboratory for Non-linear Spectroscopy
via Nello Carrara 1
I-50019 Sesto Fiorentino, Florence, Italy
and
Istituto Nazionale per la Fisica della Materia
Sezione di Firenze
via Sansone 1
I-50019 Sesto Fiorentino, Florence, Italy

T. Biagiotti
University of Florence
Department of Experimental Pathology and Oncology
viale Morgagni 50
I-50134 Florence, Italy

R. Antolini
University of Trento
Department of Physics
via Sommarive 14
I-38050 Povo, Trento, Italy

M. Olivotto
University of Florence
Department of Experimental Pathology and Oncology
viale Morgagni 50
I-50134 Florence, Italy

F. S. Pavone
European Laboratory for Non-linear Spectroscopy
via Nello Carrara 1
I-50019 Sesto Fiorentino Florence, Italy
and
Istituto Nazionale per la Fisica della Materia
Sezione di Firenze
via Sansone 1
I-50019 Sesto Fiorentino, Florence, Italy
and
University of Florence
Department of Physics
via Sansone 1
I-50019 Sesto Fiorentino, Florence, Italy

Abstract. Second-harmonic generation (SHG) is emerging as a powerful tool for the optical measurement of transmembrane potential in live cells with high sensitivity and temporal resolution. Using a patch clamp, we characterize the sensitivity of the SHG signal to transmembrane potential for the RH 237 dye in various normal and tumor cell types. SHG sensitivity shows a significant dependence on the type of cell, ranging from 10 to 17% per 100 mV. Furthermore, in the samples studied, tumor cell lines display a higher sensitivity compared to normal cells. In particular, the SHG sensitivity increases in the cell line Balb/c3T3 by the transformation induced with SV40 infection of the cells. We also demonstrate that fluorescent labeling of the membrane with RH 237 at the concentration used for SHG measurements does not induce any measurable alteration in the electrophysiological properties of the cells investigated. Therefore, SHG is suitable for the investigation of outstanding questions in electrophysiology and neurobiology.
[DOI: 10.1117/1.1895205]

Keywords: second-harmonic generation; voltage sensing; nonlinear microscopy; transmembrane potential.

Paper 04054 received Apr. 12, 2004; revised manuscript received Aug. 12, 2004; accepted for publication Aug. 27, 2004; published online Apr. 11, 2005.

1 Introduction

Measurement of the cell membrane electrical potential is of fundamental importance for understanding the electrophysiological contribution to cell signaling (see Ref. 1 and the references therein). Currently, several techniques are available for visualization of the transmembrane potential (V_M) using fluorophores that partition in the cell membrane and, based on

different physical mechanisms, report the amplitude of V_M. These dyes are traditionally classified as fast or slow, depending on their response times (for review see Ref. 2). Slow dyes (with response times longer than a millisecond) typically rely on a mechanism of voltage-induced dye redistribution and can be highly sensitive (up to 100% fluorescence change for a 100-mV variation of V_M); however, they are generally inadequate for imaging the fast dynamics of excitable cells, which occur on time scales of a millisecond or less. Currently, the most robust technique for fast imaging is based on molecular electrochromism, in which a local electric field causes shifts in the electronic energy levels of a molecule. Fluorescence measurements based on this kind of dyes have low sensitivity (2 to 10% fluorescence change for a 100-mV variation of V_M).

Some dye molecules with large hyper-Rayleigh scattering efficiency (typically styryl dyes) get aligned in the membrane and coherently produce large amounts of second-harmonic generation (SHG) signals. The possibility of using SHG to report the amplitude of the electrical potential across a membrane was first demonstrated on model membranes.[3] It was then shown that SHG intensity (normalized by ratiometric correlation to two-photon excited fluorescence) changes with the V_M in live cells.[4] An important advantage of SHG is that dye molecules that are internalized in the cytoplasm become randomly oriented and do not contribute to the SHG signal, enabling high-contrast imaging of membranes.[5,6] Because SHG is a nonlinear optical phenomenon, it can form the basis of a high-resolution nonlinear imaging scheme with all the advantages of multiphoton microscopy.[7]

An important task in the development of this technique is the quantitative characterization of SHG intensity versus V_M. Recently, the electro-optic and geometrical alignment response of an SHG membrane potential sensor in giant unilamelar vesicles have been characterized.[8,9] Millard et al. measured the voltage sensitivity of SHG from a membrane styryl dye in patch-clamped cells[10] and characterized the response of different dyes at different excitation wavelengths in the same cell line.[11] To extend the application of this technique to the investigation of outstanding problems in electrophysiology and neurobiology, it is of fundamental importance to characterize the behavior of SHG signal in different cellular systems and to determine the effects (if any) of styryl dyes on the cell membrane physiological properties.

In this paper, we used the cell patch-clamp technique to measure the dependence of the SHG sensitivity in different kinds of cells, ranging from embryonic to adult normal and tumor cells. Our measurements revealed a specific SHG sensitivity to V_M for each type of cells, with a larger sensitivity in transformed versus untransformed cells. This observation encourages the use of SHG for the investigation of the electrical activity of cells in relation to the membrane chemical features, including their alteration produced by neoplastic transformation. Measurements of the distribution of dye tilt angles in two different cell types were performed to determine whether the different SHG sensitivities could be univocally attributed to a variation of the angle geometry or the hyperpolarizability of the dye. We also demonstrate that this technique is an excellent method of investigation of the electrical activity of the cell, since fluorescence labeling of the membrane does not interfere with its electrophysiological properties.

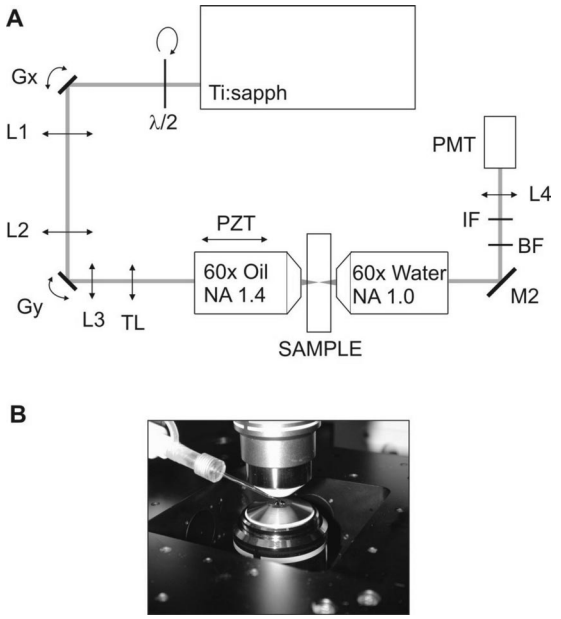

Fig. 1 Experimental setup: (a) schematic drawing of the optics of the SHG microscope and (b) close-up picture of the objectives (60× oil immersion on the bottom, 60× water immersion at the top) and patch-clamp electrode (shown on the left).

2 Materials and Methods

2.1 *Experimental Setup*

Figure 1(a) shows the experimental setup of the SHG microscope. The expanded beam of a mode-locked Ti:Sa laser with 100-fs pulse duration and 80-MHz repetition rate, model Mira 900F (Coherent, Santa Clara, California) is passed through a half-waveplate and an optical scanning system. This system is composed of two galvomirrors VM500 (GSI Lumunics, Billerica, Massachusetts) and a telescopic lens pair (L1 and L2 in the figure) that pivot the laser beam from the first galvomirror (Gx in the figure) to the second (Gy). This optical configuration was designed to implement the use of mirrors of reduced dimensions (6 mm diameter), enabling an increase of the scanning velocity with respect to conventional setups. Lenses L3 and TL pivot the laser beam in the back focal plane of the microscope objective, Plan Apo 60×/1.4 oil (Nikon, Tokyo, Japan). The SHG signal is collected in the forward direction. Since the excitation beam is focused by a high-numerical-aperture objective, the resulting SHG signal is dominantly emitted off-axis[5,6] and the collector objective, Fluor 60×/1.0 water (Nikon, Tokyo, Japan), is chosen with an appropriate numerical aperture to collect all the SHG signal. The SHG is detected with a photomultipliertube (PMT) H7710-13 (Hamamatsu, Hamamatsu City, Japan), after blocking both transmitted laser light and concurrent two-photon excited fluorescence with IR-blocking and interference filters. In the experiment, we used a motorized achromatic half-waveplate

Address all correspondence to Dr. Leonardo Sacconi. European Laboratory for Non-linear Spectroscopy, via Nello Carrara 1, I-50019 Sesto Florentino (Florence), Italy. Tel: 390554572463; Fax: 390554572451; E-mail: sacconi@lens.unifi.it

1083-3668/2005/$22.00 © 2005 SPIE

[$\lambda/2$ in Fig. 1(a)] to control the polarization of the excitation laser beam. In the measurements of SHG sensitivity on membrane potential, for each recording, two orthogonally polarized images were acquired and summed to collect signal from all the dye molecules in the membrane.[6] In the measurements of dye tilt angle, a series of images was acquired by varying the direction of linear polarization of the exciting beam over a range of 180 deg. The images were obtained with excitation wavelength of 880 nm and average laser power of 1 mW on the sample. The images dimensions are 50×50 μm with a resolution of 500×500 pixels. The integration time of each pixel is 5 μs.

The SHG microscope was integrated with a patch-clamp device AXOPATCH-1C (Axon Instruments, Inc., Foster City, California). The microneedle was positioned between the two objectives [see Fig. 1(b)] by an electronic micromanipulator InjectMan NI2 (Eppendorf, Hamburg, Germany). The SHG microscope and patch-clamp were controlled by two synchronized PCs programmed using LabVIEW software (National Instruments, Austin, Texas).

2.2 *Cells Preparation and Staining for SHG Measurements*

First, HEK 293 cells (human embryonic kidney) from clone 5, according to the method reported in Crociani et al.,[12] were transfected with *herg1* (human eag related gene) cDNA, codifying for the HERG potassium channel.[13] Briefly, the cells, cultured on 100-mm petri dishes, were transiently transfected with *herg1* cDNA cloned into *Hind*III/*Bam*HI sites of the pcDNA3.1 vector (Invitrogen) by the calcium phosphate method. Six hours before transfection, the medium was replaced once. The precipitation solution was then added to the cell cultures. The precipitation solution was 400 μl of $2\times$ balanced electrolyte solution (BES)-buffered saline [50-mM BES, 280-mM NaCl, 1.5-mM $Na_2HPO_4\cdot2H_2O$ (pH 6.96)] plus 400 μl of 0.25-M $CaCl_2$ and 36 μg of cDNA construct. The medium was replaced 15 h later and the cells were cultured in Dulbecco's modified Eagle medium (DMEM) supplemented with 10% fetal bovine serum, 1% glutamine (Euroclone) and geneticin (G418, Gibco) in air containing 5% CO_2.

Next, SH-SY5Y cells (henceforth abbreviated as SY5Y) were maintained in RPMI 1640 medium (Euroclone) supplemented with 10% fetal calf serum (FCS) (Euroclone), 1% glutamine (Euroclone) in air containing 5% CO_2, as previously described.[14]

Finally Balb/c3T3 murine fibroblasts and simian virus 40 (SV40)-transformed Balb/c3T3 cells (henceforth abbreviated as SV3T3) were grown in DMEM containing M4500 mg/L glucose (DMEM 4500) (GIBCO, Life Technologies, Italy) supplemented with 10% FCS (Boehringer Mannheim, Germany), at 37 °C in a 10% CO_2-humidified atmosphere.[15]

All cell types were seeded at 1.0×10^6 cells per 100-mm dishes and propagated every 3 days by incubation with a 0.25% trypsin solution (GIBCO). After trypsinization, cells were seeded into 24×40-mm glass coverslips and cultured as already described. After 2 days the medium was removed and supplied with low potassium solution (see later) containing the dye RH 237 (Molecular Probes, Eugene, Oregen) at a 4-μM concentration and incubated for 10 min to reach equilibration of the dye in the cell membrane. The sample was then mounted on the experimental setup for SHG measurements.

2.3 *Solutions*

1. The extracellular solution with low potassium ($E_K = -80$ mV) contained (mM): NaCl 130, KCl 5, $CaCl_2$ 2, $MgCl_2$ 2, HEPES-NaOH 10, glucose 5, with a pH of 7.4.
2. The extracellular solution with high potassium ($E_K = -30$ mV) contained (mM): NaCl 95, KCl 40, $CaCl_2$ 2, $MgCl_2$ 2, HEPES-NaOH 10, glucose 5, with a pH of 7.4.
3. The standard pipette solution at $[Ca^{2+}]=10^{-7}$ M contained (mM): K^+ Aspartate 130, NaCl 10, $MgCl_2$ 2, $CaCl_2$ 2, EGTA-KOH 10, HEPES-KOH 10, with a pH of 7.4.

2.4 *Controls on Effects of the Dye on Cell Electrophysiology*

The cells were seeded on 35-mm petri dishes and the transmembrane potential was recorded using the whole cell configuration.[16] Measurements of the membrane potential were performed in the current clamp. Pipette resistances were between 3 and 5 MΩ. Gigaseal resistances were in the range of 1 to 2 GΩ. Input resistances of the cells were in the range 2 to 6 GΩ. For data acquisition and analysis, the pClamp8 and Axoscope software (Axon Instruments, Inc., Foster City, California) and Origin (Microcal Software, Northampton, Massachusetts) were used. Comparisons were conducted between cells stained as described, but using a range of dye concentration from 0 to 12 μM.

3 Measurements and Results

3.1 *Sensitivity of the SHG*

To explore the SHG sensitivity to V_M in a wide range of cell phenotypes, we chose to carry out our experiments using the following cell lines: (1) the *herg*-transfected human embryonic kidney cell clone HEK293 (Ref. 12), (2) the neuroblastoma adrenergic clone SY5Y (Ref. 17), (3) the normal Balb/c3T3, and (4) virus-transformed SV3T3 mouse fibroblast.[15] In particular, Balb/c3T3 and SV3T3 were chosen for their suitability to explore differences of SHG sensitivity bound to changes produced by the neoplastic transformation within a properly controlled cellular model. SHG images relative to the preceding cell types, stained with RH 237, are shown in Fig. 2. Combining SHG imaging with the patch-clamp technique makes it possible to clamp the transmembrane potential of the cell and analyze the behavior of the variation of SHG intensity versus potential applied.

Bright-field images of the cells were observed to identify a suitable cell based on its morphology (cells well adhering to the glass and displaying their normal shape, depending on the cell type) and then establish on it the patch-clamp seal. During this operation a PC with LabVIEW code provided diagnostics such as seal resistance.[16] When a seal resistance of the order of 1 GΩ was obtained, the patch was ruptured and V_M was clamped at its resting value (V_{rest}). The sample was then excited with laser light and a series of SHG images were

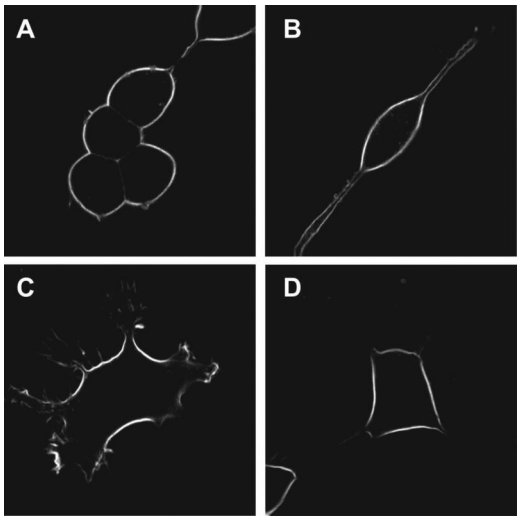

Fig. 2 SHG images of live cells stained with RH 237: (a) *herg*-transfected HEK293 epithelial cells (a cluster of cells is shown but the SHG signal arising from the regions of contact between adjacent cells is very low), (b) SY5Y neuroblastoma cell, (c) Balb/c3T3 fibroblast cell, and (d) SV3T3 cell. The images were obtained with excitation wavelength of 880 nm and average laser power of 1 mW on the sample. The images dimensions are 50×50 μm with a resolution of 500×500 pixels. The integration time of each pixel is 5 μs. Each image is the sum of two frames acquired by exciting the sample with two orthogonal polarizations.

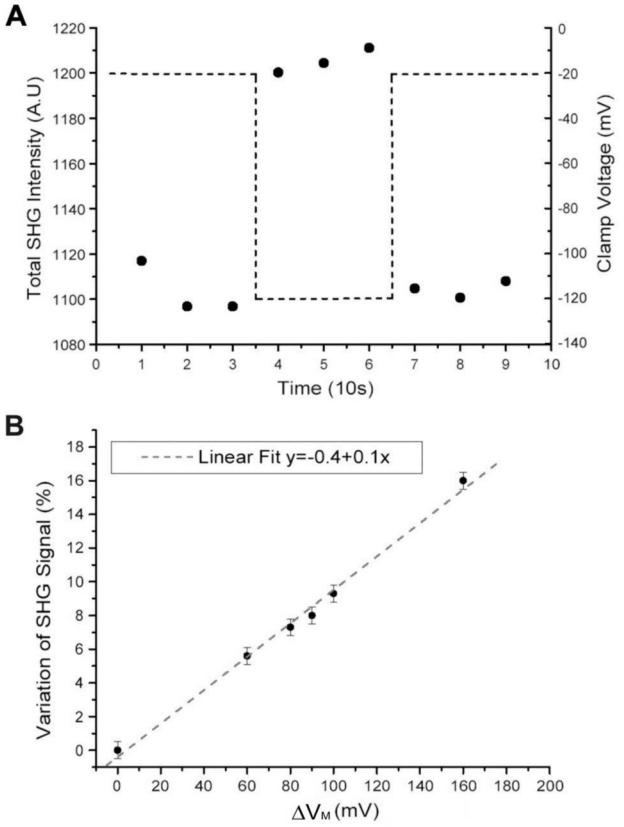

Fig. 3 SHG measurements of transmembrane potential in *herg*-transfected HEK293 cells. (a) Recording of the total SHG intensity (left axis) measured on a single HEK293 cell while switching the V_M between −20 and −120 mV using the patch clamp (the trace of voltage versus time is shown as a dashed line and the voltage scale is shown on the right axis). The total SHG signal is the integral of gray levels over the whole image acquired. (b) SHG signal change versus variation in transmembrane potential (ΔV_M). Each point is calculated from the variation in SHG measured as shown in (a). For each ΔV_M, the measurement was repeated at least five times (each on a different cell) and the mean value is reported in the graph. Error bars represent the largest deviation from the mean among all recorded data points. The dashed line is a linear regression through the data, yielding a slope of 0.10 ± 0.01%/mV ($R^2=0.997$).

acquired with a software that triggered the patch-clamp to switch between V_{rest} and $V_{\text{rest}}-\Delta V_M$ every three images. Because SHG signal arises exclusively from dye molecules partitioned into the cell membrane[6] (see also Fig. 2), it is possible to reliably quantify the signal by simply summing the grey-level of all the pixels in each image. Figure 3(a) shows the behavior of the SHG intensity (black dots) in a HEK293 cell to which a variation ΔV_M of 100 mV was imposed (dashed line). In all measurements three data points at V_{rest} were acquired before and after the ΔV_M perturbation. This enabled an evaluation of possible small variations of SHG intensity over time due to flip-flop, photobleaching, and some residual non-equilibrium diffusion of the dye into the cell membrane. When a positive or negative drift was measurable above noise in the signal before and after the ΔV_M perturbation, a correction was applied to the data by linear interpolation.[10] In the experiment shown in the figure, we measured a relative SHG intensity change of 9 ± 1%. The spread within a triplet of points acquired in one condition represents the noise of our measurements, due to different possible sources (background noise, laser power fluctuations, etc.). With the same experimental procedure, we also analyzed the relative SHG intensity changes versus voltage variation (ΔV_M). Figure 3(b) shows a linear dependence of the variation of SHG on the voltage change in HEK293 cells. The slope of a linear fit to the data [dashed line in Fig. 3(b)] is 0.10 ± 0.01%/mV. These measurements were performed on at least five different cells for each ΔV_M, enabling us to sample different cell shapes and possible spatial and temporal heterogeneities in dye incorporation.

With the same methodology, we analyzed the SHG intensity changes in SY5Y cells [Fig. 4(a)]. In these cells, the SHG change versus voltage variation was also linear [see Fig. 4(b)] but with a linear coefficient of 0.17 ± 0.01%/mV. These measurements show a significant difference between the two kinds of cells. Hypothesizing that this should be due to the difference in the membrane structure and lipid and protein composition, we measured the SHG sensitivity in other kinds of cells: Balb/c3T3 and SV3T3, where the effects of the transformation on the membrane composition are well studied.[15] In these cells, the change of SHG was measured only for a ΔV_M of 100 mV. The SHG response to this change of potential was 12 ± 1% for Balb/c3T3 and 15 ± 1% for SV3T3. Also in this case, we measured a significant difference of SHG sensitivity. Figure 5 summarizes the results from measurements in all four cell types investigated. It is interesting to notice that each cell type displays a characteristic SHG sensitivity, and the differences between cell types are significant within the precision of our measurements. The possible physical origins of these differences were investigated with measurements of the dye tilt angle in the membrane as described next.

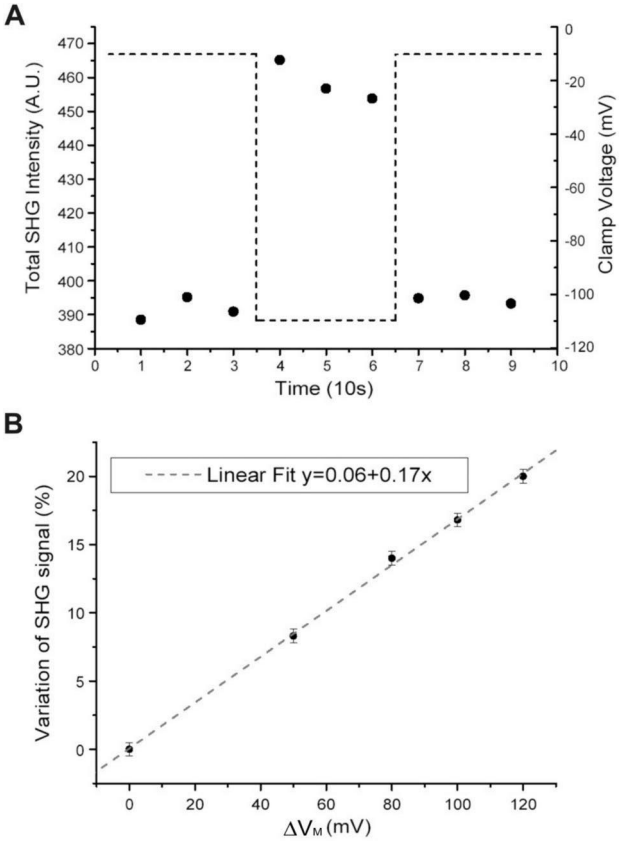

Fig. 4 SHG measurements of transmembrane potential in SY5Y cells: (a) the same type of measurement as in Fig. 3(a) is shown here on SY5Y cells and (b) see legend in Fig. 3 (b). The dashed line is a linear regression through the data, yielding a slope of $0.17 \pm 0.01\%$/mV ($R^2 = 0.999$).

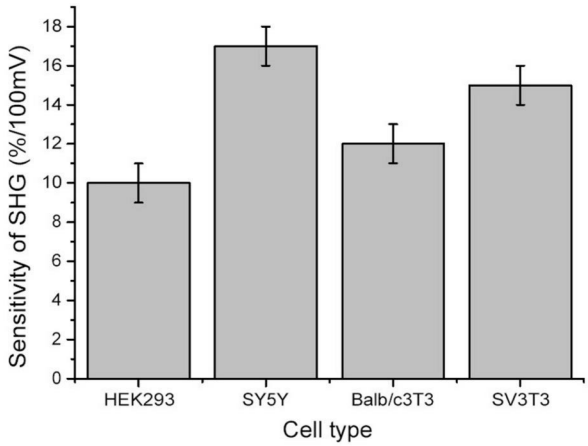

Fig. 5 Comparison of SHG sensitivity in four different cell types. Each bar represents the SHG sensitivity measured in the cell type indicated on the *x* axis. The values reported are the slope (and its uncertainty) of the regressions shown in Figs. 3(b) and 4(b) for HEK293 and SY5Y respectively. Sensitivity values for Balb/c3T3 and SV3T3 were calculated from a set of 20 measurements on each cell type with ΔV_M fixed at 100 mV; the error bars represent the largest deviation from the mean among all recorded data points.

3.2 *Measurements of the Dye Tilt Angle*

Moreaux et al.[8] developed a mathematical model enabling the determination of the dye tilt angle (with respect to the axis perpendicular to the membrane surface) from SHG measurements. In their work, Moreaux et al. used giant unilamellar vesicles (GUVs) and excited SHG with a linearly polarized beam; then, they analyzed the intensity of SHG versus the angle between the normal to the membrane surface and the exciting polarization. Taking advantage of the spherical shape of GUVs, this method enables the sampling of all dye angles from one image. In our experiments, the cells were nonspherical and the different angles between the dipole of the dye and the exciting polarization were sampled by choosing a region on the cell and imaging it with varying exciting polarizations. These measurements were performed on two cell types (HEK293 and SY5Y) clamping the membrane potential alternatively at 0 and -100 mV. A typical result of these measurements is shown in Fig. 6. For the quantitative measurements [shown in Fig. 6(b)] a rectangular region of interest of 1×40 pixels was selected with the long axis perpendicular to the surface of the membrane. This choice was operated to minimize the effects of irregularities in the orientation of the cell membrane over distances of the order of a pixel. In the direction perpendicular to the membrane, on the other hand, a larger number of pixels was chosen to collect signal from the whole membrane and compensate for small fluctuations in the cell position induced by the patch clamp electrode. The intensity data were fit using

$$\mathrm{SHG} = \mathrm{SHG}_{\parallel} + \mathrm{SHG}_{\perp}, \tag{1}$$

where $\mathrm{SHG}_{\parallel,\perp}$ are the signal components, respectively, parallel and perpendicular to the laser beam polarization:

$$\mathrm{SHG}_{\parallel} = \mathrm{SHG}_0(\langle \xi^3 \rangle \cos^3 \phi + 3/2\langle \xi - \xi^3 \rangle \cos \phi \sin^2 \phi)^2, \tag{2}$$

$$\mathrm{SHG}_{\perp} = \mathrm{SHG}_0[\langle \xi^3 \rangle \cos^2 \phi \sin \phi + 1/2\langle \xi - \xi^3 \rangle \times \sin \phi (1 - 3\cos^2 \phi)]^2, \tag{3}$$

where ϕ is the angle between the laser beam polarization and membrane normal and $\xi = \cos(\alpha)$ where α is the tilt angle of the dye.

The measurements performed on HEK293 and SY5Y cells at 0 and -100 mV did not show a significant difference in the dye tilt angle: in all cases (with $n = 7$ for each measurement), the values of ξ measured were spread over a range between 1.0 and 0.9 (corresponding to α ranging from 0 to 25 deg). The noise in these measurements arises from several factors, including variability between cells, photobleaching, possible diffusion, and flip-flop of the dye. Note also that the physical and biochemical differences existing between GUVs and living cells could give raise to systematic uncertainties on the fitted parameters. In particular, the cell membrane has an irregular profile (especially, at the subresolution level) and allows the presence of dye molecules in the two opposite lipid layers, whereas unilamellar vesicles do not pose these problems.

However, within the precision of our measurements, there was no observable dependence of the dye tilt angle on the cell type or the voltage. The implications of these observations are discussed further in the following.

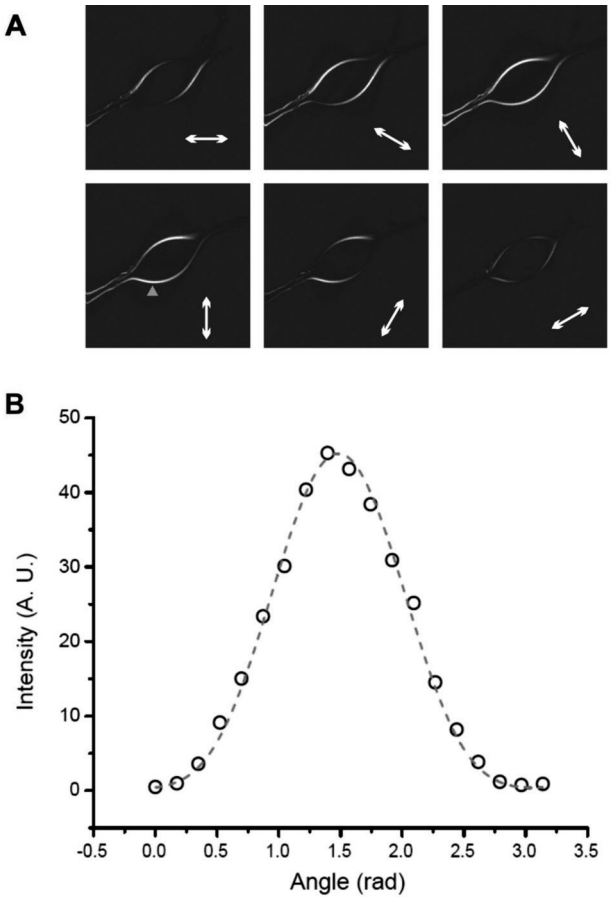

Fig. 6 Measurements of dye tilt angle. (a) Images of one cell stained with 4-μM RH237 and illuminated with light linearly polarized along the direction indicated by the arrow. The size of the images is 50×50 μm. The gray arrowhead indicates the region of interest selected for quantitative analysis as described in the text. (b) SHG intensity of the selected region of interest versus polarization angle. The dashed line represents a fit to the data using the model described in the text, yielding the following parameter: ξ=0.92±0.01, $\tilde{\chi}^2$=0.7.

3.3 *Electrophysiology Controls*

Since the styryl dye is an amphyphylic molecule that intercalates in the bilayer structure of the cell membrane, it could interfere with the normal electrophysiological properties of the cell. An effect of this kind would compromise the most attractive applications of this technique. Therefore, we performed control measurements aimed at assessing whether the dye used in this work alters the membrane physiological properties of the cells studied. In particular, we tested whether V_{rest} changes in the presence or absence of the dye. Figure 7 shows the experimental results of V_{rest} measurements obtained in the different cell types at four different dye concentrations, using an extracellular solution with low potassium. The data clearly show that, at the concentration used in the SHG measurements (4 μM), the dye does not modify the V_{rest} of the cells. We can see that significant changes in V_{rest} could be detected only at much higher concentrations (12 μM). At the highest concentration, the cells degenerated within 5 to 10 min, whereas in the range 0 to 8 μM the cells were perfectly viable for at least 30 min.

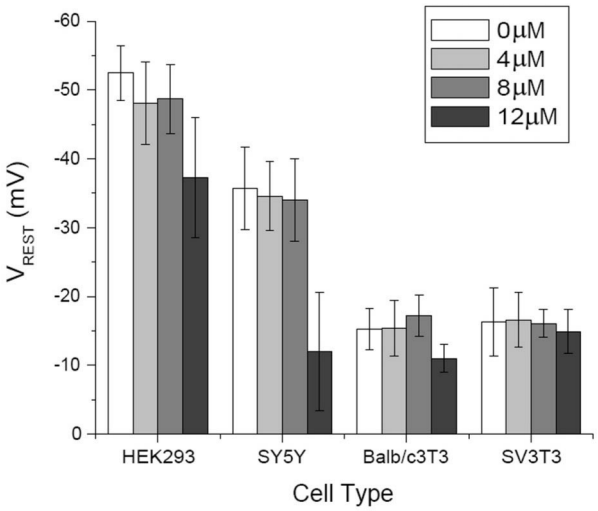

Fig. 7 Controls on the effects of RH 237 dye on cell electrophysiology; V_{rest} is shown for each cell type stained with RH 237 dye at four different concentrations, as indicated. The values shown are mean and standard deviation. Statistics were accumulated over at least 10 samples for each cell line and dye concentration.

Additionally, the changes of transmembrane potential in response to a variation of the external concentration of potassium were compared in the different cell types with 0 and 4 μM dye. Also in these measurements, there was no observable effect induced by the presence of the dye in the membrane (data not shown).

4 Discussion

Recently there has been a growing interest in the use of nonlinear optical techniques for the imaging of biological samples.[18] With respect to conventional fluorescence, these techniques offer several advantages, including higher spatial resolution, reduced photodamage of the living sample, reduced photobleaching of the dye, and increased penetration depth.

Among these techniques, SHG displays properties that make it particularly suitable for many interesting applications in life sciences.[19–21] One main area of development of SHG imaging over the past few years has been devoted to the development of methods for the optical measurement of transmembrane potential in living cells with high spatial and temporal resolution, and high sensitivity.[4,10,11] Recently, SHG has been employed to optically record the electrical activity at discrete positions on a neuron.[22] In the near future, the possibility of using SHG for imaging electrical activity on a whole cell in real time should represent a valuable noninvasive tool for the investigation of outstanding problems in neurobiology and electrophysiology.

Here, we studied the response of the SHG signal to a change in electrical potential applied with patch clamp in a variety of cell types, using the same styryl dye (RH 237) in all cells studied. This dye was selected over other commercially available dyes for the high tolerance displayed by the cells at dye concentrations suitable for optimal staining (see Fig. 2).

In other studies, the SHG sensitivities of different dyes have been compared in one cell type (neuroblastoma), highlighting large differences among the dyes investigated.[11]

We investigated whether different cell types would exhibit different SHG sensitivities to transmembrane potential. Figure 5 shows that the differences among the four cell types studied are small but significant. Interestingly, even in the same cell line (Balb/c3T3) a significant change in SHG response could be induced by infection with SV40. The effect of SV40 on these cells has been extensively studied, and the major difference between normal and infected cells has been attributed to a variation in the lipid composition of the plasma membrane.[15]

A first, very simple, interpretation of our data, therefore, consists in attributing the observed differences in SHG sensitivity mainly to geometrical differences in the dye tilt angle due to the specific packing of lipids in each cell type. For a purely electro-optic response, the relative change of the SHG intensity as a function of the transmembrane electric field can be written as[8]

$$R(E) \approx 1 + kE\xi, \tag{4}$$

where E is the transmembrane electric field, k is a parameter that depends exclusively on the electro-optical properties of the dye, and ξ is a geometrical parameter as already defined. If the observed differences in SHG sensitivity of the different cell types were to be due exclusively to electro-optic effects, then, changes in ξ of the order of 1.7 between HEK293 and SY5Y would be expected. To test this model we performed measurements of dye tilt angle. The values of ξ measured with this method ranged from 0.9 to 1.0 in both the cell types and voltages tested. The resolution of our measurements did not enable us to determine if the voltage variation (0 to -100 mV) or the biochemical differences between the plasma membranes in the two cell types indeed can cause a small but significant difference in the orientation of the dye. However, within the noise of the measurements, we can exclude variations of ξ of the order of 1.7, demonstrating that more complex mechanisms determine SHG sensitivity variations, as already described[9] in GUVs.

With respect to GUVs, living cells present the dye with a more complex environment, which can influence its response. It is very likely, therefore, that both proteins and lipids contribute to determining the differences we observed in a manner that cannot be easily quantified with simple models as attempted here. On the other hand, the complexity of factors contributing to SHG sensitivity may render this technique capable of reporting on the properties of the physical and chemical environment of the cell membrane. In fact, we notice that for the four cell types investigated the higher SHG sensitivity was displayed by the two lines of transformed cells (SY5Y neuroblastoma and SV3T3). Although a systematic investigation of the differences between normal and transformed cells is beyond the scope of this paper, this observation can be exploited for a use of SHG methods in cell screening or diagnostics. Finally, we demonstrated that the presence of RH 237 dye in the cell membrane at the concentration used in this paper does not significantly modify the electrophysiological properties of the membrane. This observation confirms that SHG microscopy is an excellent tool for the study of electrical activity in live samples.

Acknowledgments

This work was supported by grants from European Laboratory for Nonlinear Spectroscopy (LENS) Contract No. HPRI-CT-1999-00111 CE, Ente Cassa di Risparmio di Firenze (CARIFI), Associazione Italiana per la Ricerca sul Cancro (AIRC) and Ministero dell'Istruzione, dell'Università e della Ricerca (MIUR, 2002 to 2003). The authors are grateful to Prof. A. Choudhury, Prof. S. Ruggieri, and Prof. L. Calorini for helpful suggestions, and to Dr F. Bianchini for help with cells culture.

References

1. M. Olivotto, A. Arcangeli, M. Carla, and E. Wanke, "Electric fields at the plasma membrane level: a neglected element in the mechanisms of cell signaling," *BioEssays* **18**, 495–504 (1996).
2. L. B. Cohen and B. M. Salzberg, "Optical measurement of membrane potential," *Rev. Physiol. Biochem. Pharmacol.* **83**, 35–88 (1978).
3. O. Bouevitch, A. Lewis, I. Pinevsky, J. P. Wuskell, and L. M. Loew, "Probing membrane potential with non-linear optics," *Biophys. J.* **65**, 672–679 (1993).
4. P. J. Campagnola, M. Wei, A. Lewis, and L. M. Loew, "High resolution nonlinear optical imaging of live cells by second harmonic generation," *Biophys. J.* **77**, 3341–3349 (1999).
5. L. Moreaux, O. Sandre, M. Blanchard-Desce, and J. Mertz, "Membrane imaging by simultaneous second harmonic generation and two photon microscopy," *Opt. Lett.* **25**, 320–322 (2000).
6. L. Moreaux, O. Sandre, and J. Mertz, "Membrane imaging by second-harmonic generation microscopy," *J. Opt. Soc. Am. B* **17**, 1685–1694 (2000).
7. W. Denk, J. H. Strickler, and W. W. Webb, "Two photon laser scanning fluorescence microscopy," *Science* **248**, 73–76 (1990).
8. L. Moreaux, T. Pons, V. Dambrin, M. Blanchard-Desce, and J. Mertz, "Electro-optic response of second-harmonic generation membrane potential sensor," *Opt. Lett.* **28**, 625–627 (2003).
9. T. Pons, L. Moreaux, O. Mongin, M. Blanchard-Desce, and J. Mertz, "Mechanisms of membrane potential sensing with second-harmonic generation microscopy," *J. Biomed. Opt.* **8**, 428–431 (2003).
10. A. C. Millard, L. Jin, A. Lewis, and L. M. Loew, "Direct measurement of the voltage sensitivity of second harmonic generation from a membrane dye in patch-clamped cells," *Opt. Lett.* **28**, 1221–1223 (2003).
11. A. C. Millard, L. Jin, M. D. Wei, J. P. Wuskell, A. Lewis, and L. M. Loew, "Sensitivity of second harmonic generation from styryl dyes to transmembrane potential," *Biophys. J.* **86**, 1169–1176 (2004).
12. O. Crociani, L. Guasti, M. Balzi, A. Becchetti, E. Wanke, M. Olivotto, R. S. Wymore, and A. Arcangeli, "Cell cycle-dependent expression of HERG1 and HERG1B isoforms in tumor cells," *J. Biol. Chem.* **278**, 2947–2955 (2003).
13. J. W. Warmke and B. Ganetzky, "A family of potassium channel genes related to eag in *Drosophila* and mammals," *Proc. Natl. Acad. Sci. U.S.A.* **91**, 3438–3442 (1994).
14. A. Arcangeli, L. Bianchi, A. Becchetti, C. Faravelli, M. Coronello, E. Mini, M. Olivotto, and E. Wanke, "A novel inward-rectifying K^+ with a cell cycle dependence governs the resting potential of mammalian neuroblastoma cells," *J. Physiol. (London)* **489**, 455–471 (1995).
15. S. Ruggieri, R. Roblin, and P. H. Black, "Lipids of whole cells and plasma membrane fractions from Balb/c3T3, SV3T3, and concanavalin A-selected revertant cells," *J. Lipid Res.* **20**, 760–761 (1979).
16. O. P. Hamil, A. Marty, E. Neher, F. Sakmann, and F. J. Sigworth, "Improved patch-clamp techniques for high resolution current recording from cells and cell-free membrane patches," *Pfluegers Arch.* **391**, 85–100 (1981).
17. J. L. Biedler, L. Helson, and B. A. Spengler, "Morphology and growth, tumorigenicity, and cytogenetics of human neuroblastoma cells in continuous culture," *Cancer Res.* **33**, 2643–2652 (1973).
18. W. R. Zipfel, R. M. Williams, and W. W. Webb, "Nonlinear magic: multiphoton microscopy in the biosciences," *Nat. Biotechnol.* **21**, 1368–1376 (2003).
19. P. J. Campagnola, A. C. Millard, M. Terasaki, P. E. Hoppe, C. J. Malone, and W. A. Mohler, "Three-dimensional high-resolution

second-harmonic generation imaging of endogenous structural proteins in biological tissues,'' *Biophys. J.* **81**, 493–508 (2002).
20. W. R. Zipfel, R. M. Williams, R. Christie, A. Y. Nikitin, B. T. Hyman, and W. W. Webb, ''Live tissue intrinsic emission microscopy using multiphoton-excited native fluorescence and second harmonic generation,'' *Proc. Natl. Acad. Sci. U.S.A.* **100**, 7075–7080 (2003).
21. P. J. Campagnola and L. Loew, ''Second-harmonic imaging microscopy for visualizing biomolecular arrays in cells, tissues and organisms,'' *Nat. Biotechnol.* **21**, 1356–1360 (2003).
22. D. A. Dombeck, M. Blanchard-Desce, and W. W. Webb, ''Optical recording of action potentials with second-harmonic generation microscopy,'' *J. Neurosci.* **24**, 999–1003 (2004).